Spin dynamics in ultrathin film structures with a network of misfit dislocations

G. Woltersdorf[a] and B. Heinrich
Simon Fraser University, 8888 University Drive, Burnaby, British Columbia V5A 1S6, Canada

J. Woltersdorf and R. Scholz
Max Planck Institute of Microstructure Physics, Weinberg 2, D-06120 Halle, Germany

(Presented on 8 January 2004)

Using ferromagnetic resonance (FMR) and transmission electron microscopy we studied the structural and magnetic properties of lattice mismatched magnetic ultrathin multilayers of the system Au/**Fe**/Au/Pd/**Fe**(001) prepared on GaAs(001). We observed a correlation between the periodic lattice irregularities due to the misfit accommodation processes and the resulting magnetic properties of the multilayer system: In samples with a network of misfit dislocations the FMR measurements have shown that a significant part of the damping is extrinsic and caused by two magnon scattering. The angular dependence of the FMR linewidth reflects the in-plane symmetry of the dislocation arrangement. © *2004 American Institute of Physics.* [DOI: 10.1063/1.1669219]

I. SAMPLES AND MICROSTRUCTURE ANALYSIS

The metallic multilayer films studied in this article consist of Fe, Pd, and Au layers and are grown by molecular beam epitaxy on GaAs(001), see details in Ref. 1. The following Fe ultrathin films (shown in bold) in multilayer samples were studied: 20Au/**40Fe**/40Au/*n*Pd/16Fe/GaAs(001) and 20Au/**40Fe**/40Au/*n*Pd/$[\mathrm{Fe/Pd}]_5$/16Fe/GaAs(001), the integers and *n* are in monolayers (MLs). $[\mathrm{Fe/Pd}]_5$ is a $L1_0$ superlattice with five repetitions. The Fe(001) mesh is closely matched to Au(001) (-0.5% mismatch) by rotating 45° in the plane ($[100]_{\mathrm{Fe}} \| [110]_{\mathrm{Au}}$). However Pd has a large lattice mismatch of 4.4% with respect to Fe and 4.9% with respect to Au, and therefore samples with a sufficient thickness of Pd are affected by the relaxation of lattice strain. The formation of misfit dislocations in those samples was evident during the growth by reflection high energy electron diffraction fanout streak patterns on the Au(001) cap and spacer layers.[2]

A self-assembled network of misfit dislocation half loops was observed using transmission electron microscopy by plan view orientation of the layer system 90Au/9Pd/**16Fe**/GaAs(001) [cf. Fig. 1(a)]. The observed orientation and density of the dislocation arrangement resembles well the misfit dislocation networks observed by Woltersdorf[3] and Woltersdorf and Pippel[4] in epitaxially grown Au/Pd bicrystals of the corresponding thicknesses: During the growth of the first Pd monolayers on Au(001) substrates complete misfit dislocations are generated and form a rectangular network located in the Pd/Au interface. After reaching a critical thickness of 4 ML the process of gliding of substrate dislocations can no longer produce a sufficiently high density of dislocations to compensate the misfit; thus an additional generation of dislocation half loops[5] started at the top Pd layer and extended to the interface. The corresponding interference of moiré patterns and dislocation contrast phenomena treated in Ref. 4 are also recognizable in Fig. 1(a). The generation mechanisms of interface dislocations and their efficiency for misfit compensation is outlined in Ref. 6.

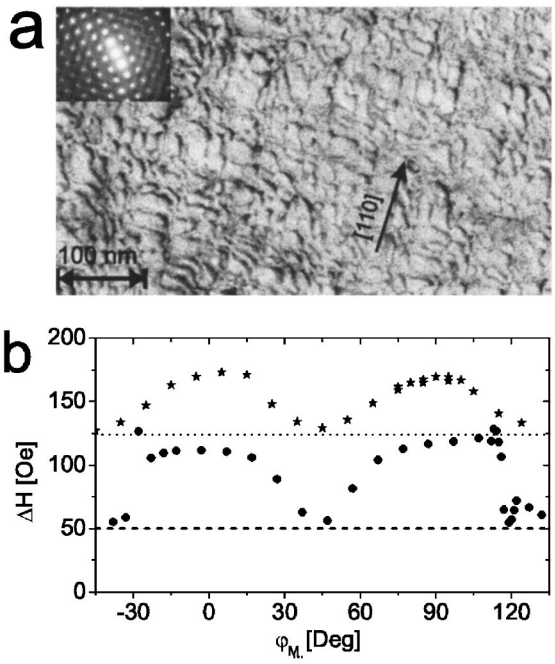

FIG. 1. **(a)** Plan view TEM image of the 90Au/9Pd/**16Fe**/GaAs(001) sample exposing the misfit dislocation network. The upper part shows the corresponding diffraction pattern. The fourfold symmetry of defects is evident in the presence of reciprocal sheets. The mean separation between dislocation lines was ~15 nm corresponding to a Fourier component of $\sim 1 \times 10^6$ cm^{-1}. The arrow is along the $[110]_{\mathrm{Au}}$ corresponding to $[100]_{\mathrm{Fe}}$. **(b)** Half width half maximum linewidth for the top **40Fe** layer in the 20Au/**40Fe**/40Au/4Pd/$[1\mathrm{Fe}/1\mathrm{Pd}]_5$/16Fe/GaAs(001) structure at 73(★) and 24(●) GHz as function of the in-plane angle φ_M of the magnetization **M** with respect to $[100]_{\mathrm{Fe}}$. The Gilbert damping contribution is indicated by the dotted lines. The discontinuities for the 24 GHz measurements are caused by spin pumping around accidental crossovers of the resonance fields (see Ref. 7).

[a]Author to whom correspondence should be addressed; electronic mail: gwolters@sfu.ca

II. SPIN DYNAMICS IN LATTICE STRAINED STRUCTURES

Magnetic relaxation was investigated using ferromagnetic resonance (FMR). The FMR experiments were carried out with 14, 18, 24, 36, and 73 GHz systems. In this article it will be shown that the effective magnetic damping is strongly enhanced in samples with a self-assembled network of misfit dislocations, and that the enhancement in the FMR linewidth, ΔH, can be described by two magnon scattering. Finally we will show that the measured dependence of two magnon scattering on the microwave frequency and the angle φ_M of the magnetization with respect to the crystalline axis allow one to identify the two dimensional Fourier components of magnetic defects. The magnetic anisotropies of the top **40Fe**(001) layer, in 20Au/**40Fe**/40Au/9Pd/16Fe/GaAs(001), and 20Au/**40Fe**/40Au/4Pd/$[\mathrm{Fe/Pd}]_5$/16Fe/GaAs(001) structures are similar to those in nearly lattice matched and dislocation free 20Au/**40Fe**/40Au/16Fe/GaAs(001) structures.[1] The main quantitative difference between the samples with a thick Pd layer, $N_{\mathrm{Pd}} \geqslant 9$ ML, and those with $N_{\mathrm{Pd}} < 5$ ML was in magnetic damping, where N_{Pd} represents the total number of atomic Pd layers in the structure. The top layer (**40Fe**) in magnetic double layers with $N_{\mathrm{Pd}} < 5$ has shown simple Gilbert damping α enhanced only by spin pumping.[1,7] α was determined from the linear frequency dependence of ΔH. The FMR linewidth in 20Au/**40Fe**/40Au/9Pd/16Fe/GaAs(001) and 20Au/**40Fe**/40Au/4Pd/$[\mathrm{Fe/Pd}]_5$/Fe/GaAs(001) samples with $N_{\mathrm{Pd}} \geqslant 9$, was very different. In these samples the FMR linewidth, ΔH, was strongly dependent on the angle φ_M [see Figs. 1(b) and 2(a)]. ΔH shows a distinct fourfold symmetry. The minima in ΔH are along the magnetic hard axis $\langle 110 \rangle_{\mathrm{Fe}}$, and the maxima in ΔH are along the easy axes $\langle 100 \rangle_{\mathrm{Fe}}$ at all microwave frequencies. The frequency dependence of the FMR linewidth ΔH along the $\langle 100 \rangle_{\mathrm{Fe}}$ and $\langle 110 \rangle_{\mathrm{Fe}}$ axes is shown in Fig. 2(b). For the magnetization along the in-plane $\langle 110 \rangle_{\mathrm{Fe}}$ directions, the FMR linewidths at 36 and 73 GHz were found to be very close to those caused by the Gilbert damping in 20Au/**40Fe**/40Au/16Fe/GaAs(001). The results are different for the FMR measurements with the saturation magnetization along the $\langle 100 \rangle_{\mathrm{Fe}}$ directions. First, the FMR linewidths are larger than those along the $\langle 110 \rangle_{\mathrm{Fe}}$ directions. Second, the microwave frequency dependence is not described by a simple linear dependence as expected for Gilbert damping. In fact the nonlinear frequency dependence [see Fig. 2(b)] resembles recent calculations by Arias and Mills's[8] of two magnon scattering in ultrathin films. A similar frequency dependence of ΔH was found recently by Twisselmann and McMichael[9] for Permalloy films grown on NiO and Linder *et al.*[10] on Fe_4V_4 superlattices.

Obviously, the anisotropic contribution to the FMR linewidth is not intrinsic. A similar FMR line broadening behavior was observed in the following Fe films (in bold) in strain relieved crystalline structures: 20Au/**40Fe**/40Pd/**16Fe**/GaAs(001), 20Au/**20Fe**/40Pd/**16Fe**/GaAs(001), 200Pd/**30Fe**/GaAs(001), and 90Au/9Pd/**16Fe**/GaAs(001). This indicates that the extrinsic damping does not depend on the Fe layer thickness and its location inside the structure, and therefore originates in the interior of the Fe film. This implies that the dislocation glide along $\{111\}_{\mathrm{Au}}$ planes propagates across the whole multilayer.

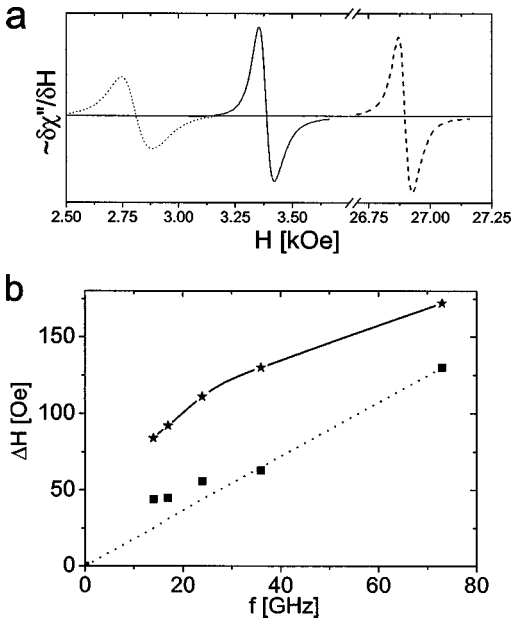

FIG. 2. **(a)** Typical FMR spectra measured at 24 GHz on a 20Au/**40Fe**/40Au/4Pd/$[1\mathrm{Fe}/1\mathrm{Pd}]_5$/16Fe/GaAs(001) sample. The left spectra were taken with the magnetization **M** in the plane: $\mathbf{M} \| [110]_{\mathrm{Fe}}$ (solid line) and $\mathbf{M} \| [100]_{\mathrm{Fe}}$ (dotted line). The right spectrum (dashed line) corresponds to the perpendicular configuration ($\mathbf{M} \| [001]_{\mathrm{Fe}}$). Note that the FMR linewidths in the in-plane configuration are anisotropic, and the narrowest line is measured in the perpendicular configuration. **(b)** Frequency dependence of the FMR linewidth, ΔH, for the top **40Fe** layer in the 20Au/**40Fe**/40Au/4Pd/$[1\mathrm{Fe}/1\mathrm{Pd}]_5$/16Fe/GaAs(001) structure along the $\langle 100 \rangle_{\mathrm{Fe}}$ ($\star$) and $\langle 110 \rangle_{\mathrm{Fe}}$ ($\blacksquare$) axes, respectively. The purpose of the solid spline fit is to guide the reader's eye. The dashed line shows the frequency dependence of the intrinsic FMR linewidth (Gilbert damping) of the **40Fe**(001) layer. The Gilbert damping in a double layer with well separated resonance fields includes the contribution by spin pumping (Ref. 7).

III. TWO MAGNON SCATTERING

In FMR the uniform mode ($q \sim 0$) can be scattered by magnetic inhomogeneities into nonuniform modes ($\mathbf{q} \neq 0$ magnons). Two magnon scattering has been used to describe extrinsic damping in ferrites[11,12] and metallic films.[13] The two magnon scattering matrix is proportional to components of the Fourier transform $A(\mathbf{q}) = \int d\mathbf{r} \Delta U(\mathbf{r}) e^{-i\mathbf{qr}}$ of magnetic inhomogeneities, where $U(\mathbf{r})$ stands symbolically for a local magnetic energy. The magnon momentum is not conserved in two magnon scattering due to the loss of translational invariance, but the energy is. In ultrathin films the **q** vectors are confined to the film plane and the magnon dispersion relation can be found in Ref. 8. The degenerate modes are given by crossovers of the magnon manifold with the energy of the homogeneous mode. The direction of magnons is usually determined by the angle ψ between the magnon vector **q** and the saturation magnetization. The value of ψ determines the magnitude q_0 of the degenerate magnon. The value of q_0 decreases with an increasing angle ψ. No degenerate modes are available for angles ψ larger than $\psi_{\max} = \arcsin[H/(H + 4\pi M_{\mathrm{eff}})]^{\frac{1}{2}}$, where H is the applied field at FMR, and $4\pi M_{\mathrm{eff}}$ is the effective demagnetizing field perpendicular to

the film surface. When the magnetic moment is inclined with respect to the film surface at angles larger than $\pi/4$ no degenerate modes are available[8] and two magnon scattering disappears. In fact, we used this condition to test the applicability of two magnon scattering for the interpretation of extrinsic damping. We would like to emphasize that all samples in this article satisfied this condition [see Fig. 2(a)]. This identifies the extrinsic damping as two magnon scattering.

The two magnon scattering process is confined to degenerate magnons which are restricted to lobes, $q_0(\psi)$, around the direction of the magnetic moment. The lobes resemble in shape the infinity symbol (∞) with its center at the origin of the reciprocal space. The effectiveness of two magnon scattering as a function of the angle of the magnetization with respect to the crystallographic axis can be tested by evaluating a simplified expression for the relaxation parameter R. R is the imaginary part of the denominator of the in-plane rf susceptibility.[8] Using the above concept of Fourier components of inhomogeneities one can write

$$R(\varphi_M) \sim \int I(\mathbf{q})\,\delta(\omega-\omega_{\mathbf{q}})\,d\mathbf{q}^3 = 2\int_{-\psi_{\max}}^{\psi_{\max}} \frac{I(q_0,\psi,\varphi_M)}{\frac{\partial\omega}{\partial q}(q_0,\psi)}\,q_0\,d\psi, \quad (1)$$

where $I(\mathbf{q}) \sim A(\mathbf{q})A^*(\mathbf{q})$. The expression $q_0/\partial\omega/\partial q$ describes a weighting parameter along the two magnon scattering lobe. For a given microwave frequency this factor is nearly independent of ψ, and therefore the whole lobe contributes to R with an equal weight. It is also interesting to note that the magnon group velocity $\partial\omega/\partial q\,(q_0,\psi)$ in Eq. (1) is proportional to the strength of dipolar and exchange fields and represents the dipole exchange narrowing of the two magnon scattering mechanism.

The maximum magnon momentum q_0 in two magnon scattering is small, just of $\sim 3\times 10^5$ cm^{-1} at 73 GHz and only $\sim 5\times 10^4$ cm^{-1} at 14 GHz. Two magnon scattering probes mostly the area around the origin of the reciprocal space.

IV. DISCUSSION

The angular and microwave frequency dependence of the FMR linewidth allows one to identify the main features of $I(\mathbf{q},\varphi_M)$. The scattering matrix originates from inhomogeneous magnetic energy. This leads automatically to an explicit dependence of $I(\mathbf{q},\varphi_M)$ on the angle φ_M of the magnetization with respect to the defect axes (in our case $\langle 100\rangle_{\mathrm{Fe}}$). The dislocations are the source of the magnetic defects, but the magnetic inhomogeneities can manifest themselves on a different length scale due to the exchange interaction and magnetoelastic effects. The angular dependence of $I(\mathbf{q},\varphi_M)$ has to satisfy the symmetry of the defects. In our case it is determined by the fourfold symmetry of the defect lines ($\{111\}_{\mathrm{Au}}$ glide planes). Each of the mutually perpendicular sets of linear defects generates a spatially fluctuating uniaxial anisotropy field. This field changes its sign when the magnetization is half way ($\varphi_M \| \langle 110\rangle_{\mathrm{Fe}}$) between parallel and perpendicular orientations with respect to the defects. A similar argument was recently used by Lindner *et al.*[10] to explain the absence of two magnon scattering along the $\langle 110\rangle$ directions on Fe/V superlattices. Therefore the following ansatz: $I(\mathbf{q},\varphi_M) = Q(\mathbf{q})\cdot\cos^2(2\varphi_M)$ is appropriate to interpret the FMR linewidth. $Q(\mathbf{q})$ is the Fourier transform of the magnetic defect distribution satisfying the fourfold symmetry of the misfit dislocation network. The frequency dependent deviations of the linewidth from sinusoidal $\cos^2(2\varphi_M)$ behavior can be accounted for by the functional form of $Q(|\mathbf{q}|,\varphi)$, where the angle $\varphi = \varphi_M + \psi$ is measured with respect to the crystallographic axis.

Angular dependent extrinsic damping created by a rectangular network of defects appears to be a common phenomenon. It was observed in our previous studies using the metastable bcc Ni/Fe(001) bilayers grown on Ag(001) substrates,[14] and Fe(001) films grown on bcc Cu(001).[15] In the Ni/Fe bilayers bcc Ni went through a major structural change going towards the stable fcc phase of Ni(001), resulting in a network of rectangular lattice defects. The angular dependence of the FMR linewidth indicated that the defect lines were oriented along the $\langle 100\rangle$ axes of Fe(001). The bcc Cu(001) layer went through a lattice transformation after the thickness of the Cu layer was larger than 10 ML. Again a strong anisotropy in ΔH was observed for the Fe(001) films grown on the lattice transformed Cu(001) substrates. The angular dependence indicated that the defect lines in Fe(001) were along the $\langle 100\rangle$ crystallographic directions. We observed this type of two magnon scattering also in half metallic NiMnSb(001) films[16] which were affected by two sets of rectangular lattice defects along the $\langle 100\rangle$ and $\langle 110\rangle$ directions. Consequently, the two magnon scattering was anisotropic, but did not disappear in any direction.

[1] R. Urban, G. Woltersdorf, and B. Heinrich, Phys. Rev. Lett. **87**, 217204 (2001).
[2] G. Woltersdorf and B. Heinrich (unpublished).
[3] J. Woltersdorf, Appl. Surf. Sci. **11/12**, 495 (1982).
[4] J. Woltersdorf and E. Pippel, Thin Solid Films **116**, 77 (1984).
[5] D. Bacon and A. Cocker, Philos. Mag. **12**, 195 (1965).
[6] J. van der Merwe, J. Woltersdorf, and W. Jesser, Mater. Sci. Eng. **81**, 1 (1986).
[7] B. Heinrich, Y. Tserkovnyak, G. Woltersdorf, A. Brataas, R. Urban, and G. Bauer, Phys. Rev. Lett. **90**, 187601 (2003).
[8] R. Arias and D. L. Mills, Phys. Rev. B **60**, 7395 (1999).
[9] D. Twisselmann and R. McMichael, J. Appl. Phys. **93**, 6903 (2003).
[10] J. Lindner, L. Lenz, K. Kosubek, K. Baberschke, D. Spoddig, R. Meckenstock, J. Pelzl, Z. Frait, and D. Mills, Phys. Rev. B **68**, 060102(R) (2003).
[11] M. Sparks, *Ferromagnetic Relaxation Theory* (Mc Graw–Hill, New York, 1966).
[12] M. J. Hurben, D. R. Franklin, and C. E. Patton, J. Appl. Phys. **81**, 7458 (1997).
[13] C. E. Patton, C. H. Wilts, and F. B. Humphrey, J. Appl. Phys. **38**, 1358 (1967).
[14] B. Heinrich, S. Purcell, J. Dutcher, K. Urquhart, J. Cochran, and A. Arrott, Phys. Rev. **64**, 5334 (1988).
[15] Z. Celinski and B. Heinrich, J. Appl. Phys. **70**, 5935 (1991).
[16] B. Heinrich, G. Woltersdorf, R. Urban, E. Rozenberg, G. Schmidt, P. Bach, and L. Molenkamp, J. Appl. Phys. **95**, 7462 (2004), these proceedings.